

See discussions, stats, and author profiles for this publication at: <https://www.researchgate.net/publication/301721764>

Infinite 3D Modelling Volumes

Conference Paper · January 2016

DOI: 10.5220/0005722002460253

CITATION

1

READS

85

2 authors, including:



Eugen Funk

German Aerospace Center (DLR)

12 PUBLICATIONS 5 CITATIONS

SEE PROFILE

All content following this page was uploaded by [Eugen Funk](#) on 18 September 2016.

The user has requested enhancement of the downloaded file. All in-text references [underlined in blue](#) are added to the original document and are linked to publications on ResearchGate, letting you access and read them immediately.

Infinite, Sparse 3D Modelling Volumes

Eugen Funk and Anko Börner

Department of Information Processing for Optical Systems, Institute of Optical
Sensor Systems, German Aerospace Center (DLR), Berlin, Germany
`eugen.funk@dlr.de`, `anko.boerner@dlr.de`

Abstract. Modern research in mobile robotics proposes to combine localization and perception in order to recognize previously visited locations and thus to improve localization as well as the object recognition processes recursively. A crucial issue is to perform updates of the scene geometry when novel observations become available. The reason is that a practical application often requires a system to model large 3D environments at high resolution which exceeds the storage of the local memory. The underlying work presents an optimized volume data structure for infinite 3D environments which facilitates i) successive world model updates without the need to recompute the full dataset, ii) very fast in-memory data access scheme enabling the integration of high resolution 3D sensors in real-time, iii) efficient level-of-detail for visualization and coarse geometry updates. The technique is finally demonstrated on real world application scenarios which underpin the feasibility of the research outcomes.

1 Introduction

Research on autonomous vehicles has become eminent in recent years. A significant driving force is the vision of autonomous transport. Cars or pillars, which can operate autonomously 24 hours a day are highly attractive for logistics and public or private transport [1]. This vision has lead to intensive research that is also emphasized by the European Commission [7].

Another fruitful area of research is the automation of production sets, where robots optimized for a single-task are carefully separated from people [4]. The future of automation lies in flexible factory floors and quick burst manufacturing processes, which can provide complex, short-life-cycle products without investing into reconfiguration of the production set.

Both research disciplines have a particular aspect in common: When it comes to simultaneous application of multiple robots, lifelong world modelling or accurate localization using optical 3D sensors becomes a critical task. Moreover, both research disciplines heavily rely on 3D sensors such as stereo cameras or laser scanners. These are the low-level interfaces between the algorithmic data analysis and the physical world. The goal is to integrate each 3D measurement from the environment, whether a recognized object, its state or its geometrical 3D shape, into a global and consistent database. Such a database aims at

supporting all other mobile platforms in navigation and scene understanding. Only when a mobile robot can localize itself with respect to walls or other static obstacles, it is able to move and to approach targeted locations.

Common 3D sensors such as laser scanners, stereo or *time of flight* cameras provide samples in \mathbb{R}^3 of the environment. The set of all given samples is usually referred to as a *point cloud*, since no structural information is provided by the sensors. The goal in perception robotics is further to process the point clouds to meaningful information, such as 3D maps, obstacles and its positions, or any other objects of interest. In fact, autonomous vehicles are able to avoid obstacles, to navigate or to pick up load only when the 3D samples have successfully been processed to an application specific model. The information processing challenge is aggravated by the circumstance that the sensors deliver large 3D point datasets. A stereo camera, working at VGA resolution (640×480) at 10 frames per second delivers 3 million 3D points per second. Therefore, in order to integrate all measurements over multiple days or even years, a highly efficient 3D database is required. Only then it is possible to deploy a long-term operating robot capable of surface extraction, or object recognition.

Today, intensive research is undertaken by the robotics community focusing on the 3D perception. Issues such as strong noise, huge data sets and restricted computation resources make the task particularly challenging. Furthermore, 3D modelling via stereo cameras is remarkably difficult since variations in light or object surface properties lead to non-gaussian errors and hamper the modelling processes. Stereo cameras for autonomous vehicles are, however, favourable since no interference between other sensors and no a priori infrastructure in the application domain is required. Improvements in this domain are expected to enable autonomous vehicles to operate in factories and in public environments with a strong impact on the production efficiency, traffic safety, logistics and public transportation.

When processing 3D points from range sensor in general, it is an accepted practice to group the 3D samples into small cubic volumes, *voxels*. This enables redundant data to be removed and the memory layout to be structured efficiently since the voxel resolution is defined by the user a priori.

The underlying work presents a voxel-based database approach which makes it possible to create and to store 3D models and maps of unlimited size and to access voxels efficiently by a given 3D coordinate (x, y, z) . In contrast to standard approaches, where the modeling volume is bounded, the presented technique enables the extension of the volume dynamically. This is of particular interest for all 3D robotics applications, where the size of the environment the robot needs to operate upon is now known a priori.

Section 2 introduces details from the state of the art research on 3D modelling via voxels, aligned to the proposed approach. Section 3 states the research objectives investigated in this work. In Section 4 the proposed methodology is presented, which clarifies the novel data structure (Sec. 4.1) and its implication on the voxel query speed using 3D coordinates (Sec. 4.2). Section 5 introduces the 3D modelling framework. A standard approach is discussed critically

with respect to its limitations and an improved technique is proposed. Section 6 demonstrates the application of the voxel database and the 3D fusion technique from range (RGB-D) camera images. Finally, concluding remarks and aspects for further research are given in Section 7.

2 Literature Review

Random access of a 3D point by a given coordinate (x, y, z) is a difficult task, since the search complexity usually depends on the number of samples in the database. Grouping the data to cubic cells on a regular grid and storing them in a 3D array enables very fast access and has been the state of the art technique for many years. The reason is, when the resolution r of a volume is known, e.g. $r = 1\text{cm}$, then the access to the corresponding voxel coordinate $x = 13\text{m}$ is performed by computing its index i in the storage array $i = x/r = 1300$. The drawback of this approach is that the memory requirements grow with the cube of the space size. Representing a dense volume $100 \times 100 \times 100 \text{ m}^3$ at 1cm resolution, would require 3.7 TB of memory when using 32 bit data inside each cell. A common approach to this issue is to structure the occupied cells with a hierarchical *octree*, where each node (cube) contains eight cubes of smaller sizes ([9], [12]). When searching a voxel given a coordinate (x, y, z) , the tree is traversed starting from the largest top node, as shown in Figure 1. This means, that the number of hierarchy levels increases the number of path checks and thus directly affects the access speed of a voxel. Each time an arbitrary voxel is addressed, either when iterating or performing random access, it is necessary to traverse the full height of the octree. In short, the search technique in octrees suffers from the access complexity $\mathcal{O}(d)$ with d being the octree-depth.

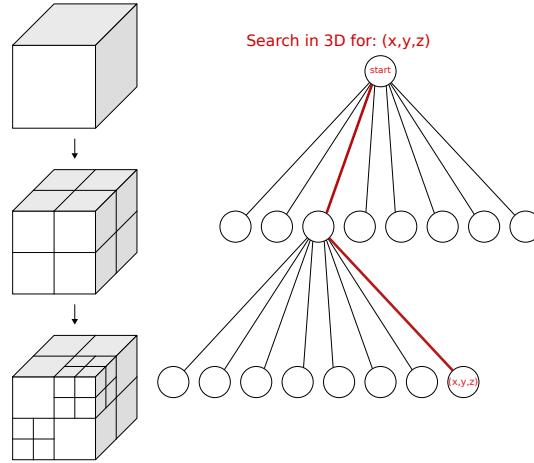


Fig. 1: Illustrated octree structure and the data access path (red), when searching for a voxel at coordinates (x, y, z) .

Teschner [18] proposed to apply a hash-map to achieve constant time access $\mathcal{O}(1)$ to sparse voxels. In principal, a coordinate (x, y, z) is encoded to a hash index which is used for direct data access. Another benefit of hash based databases, is that the amount of data can be theoretically infinite. This further allows to store data at nearly arbitrary resolution enabling huge models to be managed which is only limited by the capacity of the physical memory. However, generating unique hash values is a difficult if not an impossible task. The goal is to avoid generating a hash value representing different coordinates [18].

Niessner [17] approached the *collision issue* by storing also the coordinate of a voxel and by grouping voxels with same hash values to *buckets* (See Figure 2). When a voxel is found by a hash value, which does not correspond to the searched coordinate, the next element in the bucket is accessed.

However, direct voxel hashing does not allow to apply level of detail (LOD) visualization or multi scale 3D modelling which is favourable when low and high resolution processing is required. In fact, LOD data structure enables to perform coarse rendering depending on the distance to the virtual camera and coarse 3D modelling depending on the expected error of a measurement [8]. Practically speaking, when it is known that the covariance of a 3D sample covers several meters, it is not necessary to perform high resolution modelling on a 1cm grid. The efficiency of the hash maps and the LOD capability of octrees motivated the development of a hybrid hashed octree, which is discussed next. We combine the hashing technique from Teschner [18], approach the collision issue similarly to Niessner but reference entire octrees by a hash index instead of small voxels.

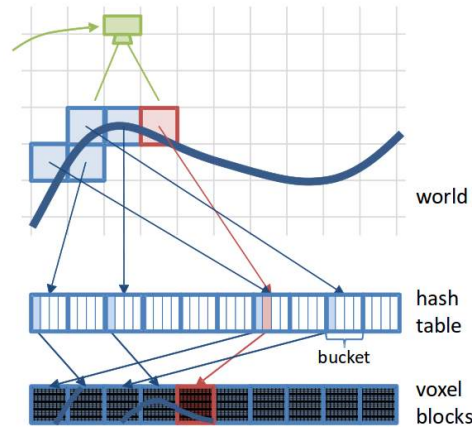


Fig. 2: Niessner [17] applied a hash table for voxels. Voxel coordinates leading to the same hash key are grouped to buckets.

3 Research Objectives

The first research objective is the development of voxel database to enable storage of geometrical models or 3D maps of unlimited size. The hash search collision issues need to be addressed in order to guarantee correct voxel access given a coordinate query.

The second objective is the integration of multiple levels of detail. Since direct voxel hashing does not enable to query larger spatial groups of voxels, the objective is to use the hashing technology for entire octrees covering larger volumes. This would combine efficient data access known from hash tables and the favourable LOD data access scheme known from octrees.

The third research objective is the development of a 3D modelling technique applied upon the proposed voxel database. Motivated by the application in autonomous vehicles, successive 3D measurements need to be used for successive model updates. That means that each new point cloud from a camera frame is expected to update an existing geometrical model. Thus, a recursive technique is required for this task to be accomplished in real-time. A crucial aspect is the suppression of noise and outliers from the input data.

Section 4 presents the developed octree hashing technique, and the hash table applied for storage and search of hash indices. In Section 5 the proposed voxel database is applied for successive 3D modelling. In contrast to the work from [17], the proposed work incorporates an adaptive noise suppression technique enabling low cost and low power range sensors such as stereo cameras to be applied.

4 Methodology

The hashing technique, inspired by [18] is extended to octrees. The fundamental part of the technique is the storage and search of arbitrary data elements indices via a hash map [10]. Finally, the performance of the developed hashed octree framework is compared to a standard octree approach and the sparse octree technique from [12].

4.1 Hash Indexing

We propose to combine octrees with a hash table (Figure 3) leading to sparse voxel representation. The hash table is used to access the top level root nodes which further contain an octree in itself. Since the internal octrees are constructed with low depth (e.g. $d = 2$), this significantly decreases the access time compared to standard octrees. To access the voxel at central index coordinates (x, y, z) , we begin by computing the rootKey

```
int rootKey[3]={x^((1<d)-1),
               y^((1<d)-1),
               z^((1<d)-1)};
```

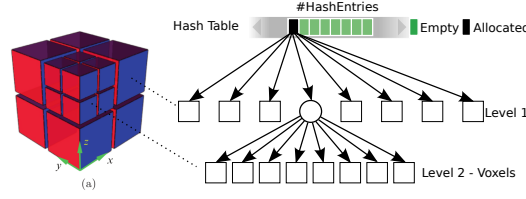


Fig. 3: Multiple octrees are stored independently referenced by a hash.

where d is the depth of the internal octree, $\&$ and \sim denote, respectively, bit-wise AND and NOT operations. At compile time, this reduces to just three hardware AND instructions. The shift by d makes sure that the coordinates (x, y, z) are represented by coarser values. For instance, applying an internal octree of depth $d = 3$ with $2^d = 8$ subdivision nodes in each dimension the space is divided in coordinate ranges $\{[0, 7], [8, 15], \dots\}$. This process is illustrated in Figure 4. For example, the operation $(1 \ll 3) - 1$ results in first three bits set to one. Negating the same, leads to five one-bits and three zero bits, as shown in the illustration of $\sim((1 \ll 3) - 1)$. Similar to [18], the rootKey is further processed to a hash using large prime numbers.

```
unsigned int rootHash=((1 << N)-1)&
    (rootKey[0]*73856093^
    rootKey[1]*19349663^
    rootKey[2]*83492791);
```

Here, N is the constant bit-length of the hash, the three constants are large prime numbers, \wedge is the binary XOR operator and \ll is the bit-wise left shift operator. Since the hash is imperfect, collisions occur so that multiple different coordinates are mapped by the same hash. The size of the hash map N influences the collision probability. In our experiments N was set to 32 bit leading to 70cpm (collisions per million of distinct coordinates). A drawback of the hash is that it is not well suited for negative coordinates. Thus, when negative values in (x, y, z) are processed to a hash, the number of collisions increases by up to 50%. Such high rates require countermeasures which are undertaken by additional octree place holders (green cells in Figure 3). Each octree reference stores also its coordinate. When an octree is searched by coordinate given by the user, the resulting octree is validated. If the validation fails, next cell in the reference list is checked. Finally, an octree root node enclosing the searched coordinate

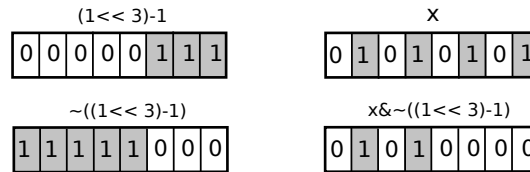


Fig. 4: Illustration of the key generation steps.

is traversed to give the targeted voxel. The linear search within a hash block slightly reduces the performance since the hash keys are small and fit into the Level-1 cache of the CPU.

4.2 Hashed-Octree Performance

We have compared the performance of the proposed hashed-octree with a standard octree implementation and the recent work from [12]. The second column in Table 1 shows the achieved random access times for each approach. The third column contains the best achievable resolution applying the corresponding technique. For example, using an octree with depth $d = 16$, the maximum number of voxels is 32768^3 which corresponds to $(327m)^3$ when each voxel represents a box volume of $1cm^3$. While octrees are usually limited, the hashed octree approach is not. In theory, geometrical models of infinite size can be represented by the proposed technique. However, direct storage of the voxels in the computer memory is not practical and streaming out of core techniques [2] need to be considered.

Table 1: Octree access time comparison

Method	Access time	Max. resolution
Octree ($d = 16$)	$6.43 \mu s$	$32768^3 (327m)^3 @ 1cm$
Octree [12] ($d = 16$)	$2.55 \mu s$	$32768^3 (327m)^3 @ 1cm$
Hashed-Octree ($d = 2$)	$0.45 \mu s$	∞

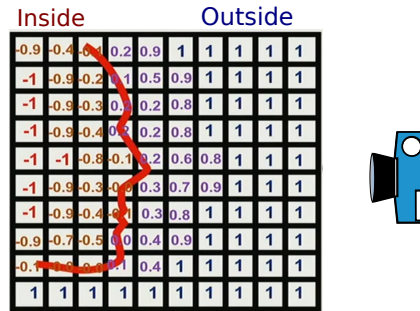


Fig. 5: Implicit shape representation by the zero level set of voxels.

5 Application to 3D Modelling

The final goal of the presented research work is the application of the developed hashed octree techniques for successive 3D modelling. When a new measurement, a 3D point cloud, becomes available from the range sensor, the goal is to update the existing 3D model as fast as possible. Several years ago Curless and Levoy [6] proposed a volumetric update approach, applying the Nadaraya Watson regression technique [16] for successive volume updates from streaming range measurements. In contrast to standard surface modelling techniques with polygons, the surface is represented by a zero level set. In principle, each voxel contains a positive or a negative scalar value indicating its location inside or outside of an object. Figure 5 outlines this concept. When a surface is observed by a range camera, the volumetric model divides the full space into interior and exterior areas. The goal is further to assign correct values to the voxels around the surface in order to approximate the shape as accurate as possible.

During the reconstruction process each pixel in the camera image is processed to a 3D point $p \in \mathbb{R}^3$. The ray between the camera centre and the 3D point is traversed updating the implicit value of each voxel lying on the ray. In order to increase the computation speed and to reduce the memory overhead, only voxels within a small distance away from p are updated. Figure 6a shows the updated neighbouring voxels in red and the sample p as a dark red circle. As mentioned before, it is assumed that voxels inside an object receive a negative and outside-voxels a positive scalar value. The distribution of the positive and negative values is described by a *signed distance function* (SDF) in Figure 6b. The goal is finally to incorporate the SDF into the voxel model updating existing values.

As illustrated in Figure 6b), each voxel receives a weight decreasing with the distance r away from the sample p . This represents the certainty of the SDF value f_i around p . Given the SDF function values f_i and its weight w_i , the existing voxels along the ray and around the sample p are updated following eq. (1). The new state ($k+1$) of the i -th voxel is computed from its previous weight w_i^k and its previous implicit value f_i^k also incorporating the novel measurements

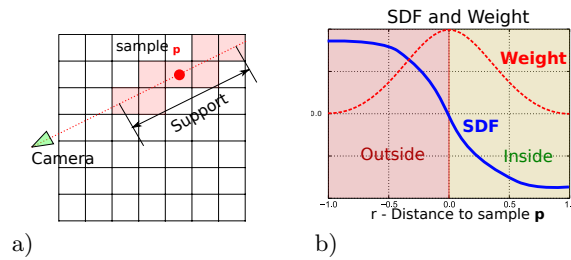


Fig. 6: a) Range of influenced voxels from a 3D sample p . b) The signed distance function applied and its weight over the distance away from the sample p .

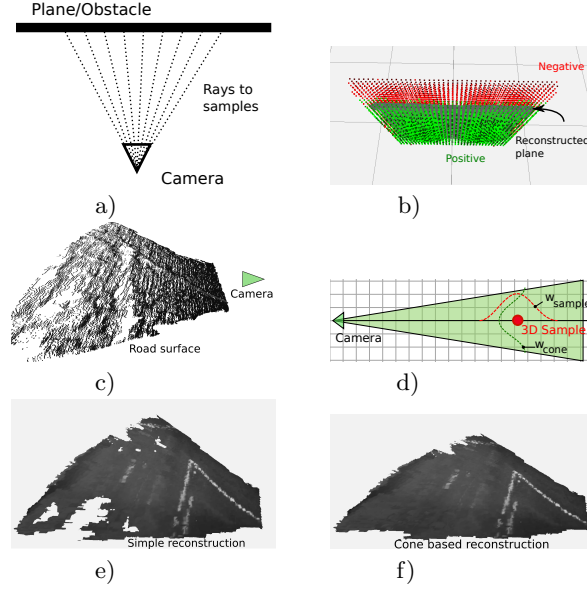


Fig. 7: a) Camera faces a wall in a synthetic setup, b) resulting voxel values, c) point cloud from a camera observing a road, d) the proposed cone fusion concept, e) mesh reconstruction of the road segment with the standard Curless & Levoy technique, f) mesh reconstruction with the proposed cone fusion technique.

w_i and f_i .

$$f_i^{k+1} = \frac{f_i^k \cdot w_i^k + f_i(r) \cdot w_i(r)}{w_i^k + w_i} \quad (1)$$

$$w_i^{k+1} = w_i^k + w_i(r)$$

Where r is representing the distance away from p . The weights follow the Gaussian distribution

$$w_i(r) = w_i^{sample} = e^{-\lambda r} \quad (2)$$

where λ is set to $\lambda = \frac{-r_{max}}{\ln(0.1)}$ which gives a weight of 0.1 at the boundaries of the SDF support. Figure 7a shows a simple synthetic scene, where a range camera faces a wall. A ray is traversed through each camera pixel and its intersection point with the plane is integrated into the 3D model as a sample. After the fusion operation (1) is applied, the voxels in front of the plane receive positive and voxels behind the wall receive negative values. This is shown in Figure 7b. Because of the simplicity of this technique, it is being applied in several 3D modelling frameworks [17, 5, 13]. However, this technique does not consider the sample sparsity and scale of the measurement errors. In cases when a wall is far away from the camera, its sample distribution is very sparse. In such a case, two neighbouring pixels in a range camera represent samples which are far away

from each other (see point cloud in Figure 7c). This leads to holes in a volume grid and in the reconstructed surface, which are not recovered by the algorithm (Figure 7e). Thus, consistent 3D modelling of surfaces is not possible when the standard technique is applied.

In order to prevent this, the technique from Curless and Levoy is extended to cones. The width of the cone is small close to the camera and large when the distance is increased (Figure 7d). Furthermore, the weights w_i are extended to

$$\begin{aligned} w_i^{full} &= w_i^{sample} \cdot w_i^{cone} \\ w_i^{cone} &= e^{-\lambda_c r_c} \end{aligned} \quad (3)$$

with r_c as the distance of the i -th voxel orthogonal to the ray. Similar to (2) λ_c is set to give 0.1 at the boundary of the cone, which is however not a critical parameter.

This extension is the main difference of the presented 3D modelling approach compared to the state of the art methods. Figures 7e-f show the effect of cone fusion on 3D samples acquired from a road surface. While the application of the standard fusion technique is likely to produce holes caused by sparse samples and noise, the presented approach still achieves consistent surfaces.

Note, that the recursive nature of the update process has a linear time complexity and is not affected by the size of the 3D model. Moreover, the voxel updates (1) inferred by each sample can be performed in parallel which further increases the computation efficiency of the technique.

Section 6 discusses the application of the technique on realistic datasets from a multi view high resolution UAV-set-up and a mobile stereo system mounted on a vehicle.

6 Experiments

The cone based 3D fusion technique with hashed octrees is demonstrated on two different applications. In the first application a UAV with a high resolution camera flew around a chapel. The images have been processed by a multi view software similar to [19]. In principle, each image is compared with all other images and similar point features (SIFT [14]) are matched. After estimating the trajectory with a *bundle block adjustment* [15] technique, the images have been processed by a multi view stereo matching algorithm from [11]. Finally, the obtained depth images for each camera frame are integrated into a global 3D model via the proposed 3D fusion technique. Figure 8 shows one of the acquired camera images (a) and the resulting 3D model (b). The full model consists of 167 millions of voxels, which has been acquired from 450 image frames. The resolution of the scene was set to 0.1m. Note, that the holes are caused by occlusions and areas which have not been observed by the UAV camera during the flight. These often relates to the ground under the trees, or the ground in the backyard of the chapel occluded by the walls.

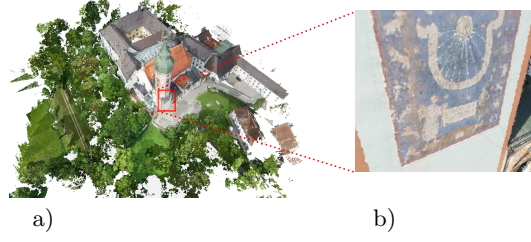


Fig. 8: a) Obtained 3D model from UAV at 1cm resolution, c) enlarged view on the chapel tower.

The second application uses a stereo camera system in combination with an inertial measurement unit (IMU). This enables to obtain the six degrees of freedom (6dof) pose of the camera in real time. This set-up is of particular interest for a wide range of indoor applications such as inspection, autonomous transport or logistics. More details about the hardware and software of the real time localization system can be found in [3]. Again, the stereo images are processed to dense disparity images [11]. The trajectory provided by the IMU+stereo system and the disparity images are directly used for 3D fusion. Figure 9 shows a point cloud (a) and the resulting 3D model (b) when the cone based 3D fusion using the hashed octree is applied.

The presented results clearly show that the developed technique is capable of handling large data sets and to process them to simplified 3D models in linear time depending on the number of 3D samples. It has been observed that the multi view 3D reconstruction point clouds suffer from less noise and errors than the real time stereo depth images. The reason is that when multiple images from a single object are available, each pixel in each depth image contains multiple depth hypotheses. This enables the optimization of the depth consistency and to increase the overall 3D reconstruction quality dramatically. As for the stereo data, the standard 3D fusion technique [6] lead to a high number of holes and artefacts in the final model. Only the cone fusion approach achieved smooth and consistent surfaces.

When the standard 3D fusion technique from [6] is applied, the algorithm achieves a runtime performance of 500ms for a single VGA (640×480) depth image on a standard desktop PC with 16 cores. After extending the algorithm to the cone fusion approach, the support width of the SDF depends on the distance between the camera and centre and p . This increases the runtime by about 20%. The worst case run time (in seconds) for a single frame via cone fusion can be estimated a priori via

$$t_{frame} = \frac{n_{res} \cdot p_{sup} \cdot r_{sup}^2}{4} \cdot t_v \quad (4)$$

with n_{res} as the resolution of the image (e.g. $640 \times 480 = 307200 = n_{res}$), p_{sup} is the width of the support around a sample (see w_{sample} Fig. 7d), and r_{sup} as the maximal width of the cone in voxels (Fig. 7d). The value $t_v = 0.45 \cdot 10^{-6}$

represents the time required to access a single voxel in the database as shown in Table 1.

Compared to the recently proposed GPU driven 3D fusion technique from Niessner [17], the runtime performance is significantly lower. Niessner reported processing times around 15ms, which is possible when the data is cached in the internal GPU memory. In contrast to this, our method focuses on multi-threading and distributed computing which enables to obtain 3D models even when low power and low cost sensors are set-up on vehicles and the raw data is sent to a cloud computer. This strategy enables to develop a server-client architecture where the autonomous vehicles communicate with a central server and update the local environment map from a single consistent source.

7 Conclusion and Outlook

A highly efficient data structure for voxel based 3D geometry has been presented. The approach enables to model arbitrary geometries and to modify them dynamically, for instance when new 3D measurements become available from a mobile robot. The technique is fundamental to all long time operating robotic systems which are expected to interact with an unknown environment.

An advanced 3D modelling technique has been presented and applied on the 3D voxel database. The application enables very large environments to be modelled and to create high resolution maps.

Future research will focus on the integration of loop-closing localization algorithms. Another aspect of future developments will cover the extension of the presented framework to a cloud computing architecture. Low level communication with sensors, consistent global mapping and client based visualization will be targeted. The mid term goal of the project is an ubiquitous framework focusing on 3D object detection, 3D mapping and visualization of huge 3D scene.

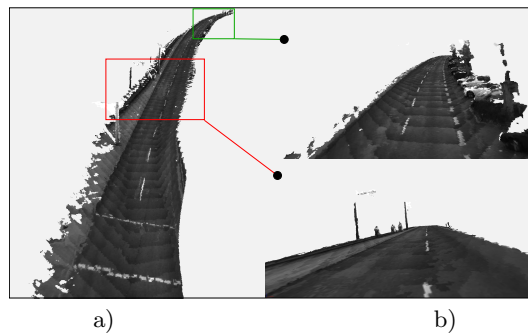


Fig. 9: a) Point cloud from stereo, b) modelled surface of the road.

References

1. [H. Andreasson, A. Bouguerra, M. Cirillo, D. Dimitrov, D. Driankov, L. Karlsson, A. Lilienthal, F. Pecora, J. Saarinen, A. Sherikov, and T. Stoyanov. Autonomous transport vehicles: Where we are and what is missing. *Robotics Automation Magazine, IEEE*, 22\(1\):64–75, March 2015.](#)
2. [J. Baert, A. Lagae, and P. Dutré. Out-of-core construction of sparse voxel octrees. In *Proceedings of the 5th High-Performance Graphics Conference, HPG '13*, pages 27–32, New York, NY, USA, 2013. ACM.](#)
3. [D. G. D. Baumbach and S. Zuev. Stereo-Vision-Aided Inertial Navigation for Unknown Indoor and Outdoor Environments. In *Proceedings of the International Conference on Indoor Positioning and Indoor Navigation \(IPIN\), 2014*. IEEE, 2014.](#)
4. [K. Bekris, R. Shome, A. Krntiris, and A. Dobson. Cloud automation: Precomputing roadmaps for flexible manipulation. *Robotics Automation Magazine, IEEE*, 22\(2\):41–50, June 2015.](#)
5. [M. G. Chajdas, M. Reitinger, and R. Westermann. Scalable rendering for very large meshes. *WSCG 2014, International Conference on Computer Graphics*, 2014.](#)
6. [B. Curless and M. Levoy. A volumetric method for building complex models from range images. In *Proceedings of the 23rd Annual Conference on Computer Graphics and Interactive Techniques, SIGGRAPH '96*, pages 303–312, New York, NY, USA, 1996. ACM.](#)
7. [EUC. FP7-Transport, Research supported by the European Commission. <http://bit.ly/1btLACw>, 2015. Accessed: 2015-09-22.](#)
8. [M. S. Floater and K. Hormann. Surface parameterization: a tutorial and survey. In N. A. Dodgson, M. S. Floater, and M. A. Sabin, editors, *Advances in Multiresolution for Geometric Modelling*, Mathematics and Visualization, pages 157–186. Springer, Berlin, Heidelberg, 2005.](#)
9. [S. F. Frisken, R. N. Perry, A. P. Rockwood, and T. R. Jones. Adaptively sampled distance fields: A general representation of shape for computer graphics. In *Proceedings of the 27th Annual Conference on Computer Graphics and Interactive Techniques*, pages 249–254. ACM Press/Addison-Wesley Publishing Co., 2000.](#)
10. [Google inc. Google sparse hash, ver1.5. <http://goog-sparsehash.sourceforge.net/>, 2015. Accessed: 2014-09-26.](#)
11. [H. Hirschmuller and D. Scharstein. Evaluation of stereo matching costs on images with radiometric differences. *IEEE Transactions on Pattern Analysis and Machine Intelligence*, 31\(9\):1582–1599, 2009.](#)
12. [A. Hornung, K. M. Wurm, M. Bennewitz, C. Stachiss, and W. Burgard. OctoMap: An efficient probabilistic 3D mapping framework based on octrees. *Autonomous Robots*, 2013.](#)
13. [S. Izadi, D. Kim, O. Hilliges, D. Molyneaux, R. Newcombe, P. Kohli, J. Shotton, S. Hodges, D. Freeman, A. Davison, and A. Fitzgibbon. Kinectfusion: Real-time 3d reconstruction and interaction using a moving depth camera. In *ACM Symposium on User Interface Software and Technology*. ACM, October 2011.](#)
14. [D. G. Lowe. Distinctive image features from scale-invariant keypoints. *Int. J. Comput. Vision*, 60\(2\):91–110, Nov. 2004.](#)
15. [P. Moulon, P. Monasse, and R. Marlet. Global fusion of relative motions for robust, accurate and scalable structure from motion. In *The IEEE International Conference on Computer Vision \(ICCV\)*, December 2013.](#)

16. E. A. Nadaraya. On estimating regression. *Theory of Probability & Its Applications*, 9(1):141–142, 1964.
17. M. Nießner, M. Zollhöfer, S. Izadi, and M. Stamminger. Real-time 3d reconstruction at scale using voxel hashing. *ACM Transactions on Graphics (TOG)*, 2013.
18. M. Teschner, B. Heidelberger, M. Mueller, D. Pomeranets, and M. Gross. Optimized spatial hashing for collision detection of deformable objects. *Proceedings of Vision, Modeling, Visualization (VMV 2003)*, pages 47–54, 2003.
19. C. Wu. Visualsfm: A visual structure from motion system. <http://ccwu.me/vsfm/>, 2011. Accessed: 2015-08-30.